Multiple-Quantum NMR Study of the Distribution of Benzene in NaY Zeolite

J. G. Pearson,† B. F. Chmelka,‡ D. N. Shykind,§ and A. Pines*

Department of Chemistry, University of California at Berkeley and Materials Sciences Division, Lawrence Berkeley Laboratory, Berkeley, California 94720 *(Received: April 13, 1992; In Final Form: July 2, 1992)*

We have used multiple-quantum NMR to measure the apparent spin network size as a function of excitation time of NaY zeolite samples containing varying amounts of benzene. Behavior observed at low concentrations of benzene was consistent with the presence of isolated clusters of benzene molecules in the supercages, with a statistical distribution of benzene molecules between supercages. Behavior observed at high concentrations of benzene was consistent with the presence of weakly coupled clusters of benzene molecules, with a uniform distribution of benzene molecules between supercages.

Introduction

The dispersion and adsorption of hydrocarbons within synthetic zeolites are of great interest owing to the selectivity imposed by the molecular sieve function of the various zeolite structures. For example, knowledge of an adsorbate's distribution in a zeolite is important in understanding molecular transport and catalysis in molecular sieves and in the use of the same as superlattice hosts in the fabrication of quantum-effect devices. Faujasite-type zeolites are of particular interest due to their high free volume and large aperture dimensions suitable for adsorption of aromatic molecules.

Benzene has been used as a molecular probe for the study of guest/host interactions, adsorption properties, and guest dynamics in zeolite systems under a variety of experimental conditions.[1-14] The relative simplicity and small size of the benzene molecule have made it a popular choice for the study of aromatic species in X- and Y-type zeolites.[1-8,12-14] The molecular dynamics of benzene in NaX and NaY zeolites have been studied using pulsed field gradient and deuterium NMR,[4,5,8] and the treatment dependence of benzene adsorption and distribution in NaY zeolite has been investigated by ^{129}Xe NMR.[13,14] In addition, the occupation of specific adsorption sites has been observed directly using neutron diffraction techniques.[7] These studies suggest a model for the adsorption and diffusion of benzene molecules within a faujasite-type zeolite. Benzene molecules appear to occupy two types of sites, cationic sites (S_{II}) on the walls of the supercage and less favorable window (W) sites in apertures between adjacent supercages. Motion of adsorbed benzene is dominated by rapid rotation about the molecule's 6-fold axis and by hops between adsorption sites. This behavior is consistent with results from separate molecular dynamics calculations.[11]

Benzene adsorbed in NaY zeolite may be distributed in essentially three different ways: uniformly, with equal numbers of benzene molecules in each supercage; randomly, with varying numbers of benzene molecules in each supercage; or in aggregates, whereby benzene molecules cluster preferentially into a small number of the available supercage cavities. Earlier observations using ^{13}C NMR[2] are consistent with either uniform or random distributions of benzene between the zeolite supercages, as shown in Figure 1a,b for a bulk loading of one molecule per supercage. A more recent study using small-angle neutron diffraction[6] suggested the existence of large molecular aggregates at the relatively low bulk loading of two molecules per supercage, as depicted in Figure 1c. We have used multiple-quantum NMR (MQ NMR) to establish the distribution of benzene molecules in NaY zeolite cavities by investigating a series of NaY samples containing different concentrations of benzene. MQ NMR permits the average number of dipole–dipole coupled protons in each zeolite supercage to be determined, thereby measuring the average number of benzene molecules occupying each NaY cavity. This method also enables the relative dipole–dipole coupling magnitudes, and thus the relative distances, to be calculated between groups of protons within the sample.

Experimental Section

The commercial NaY zeolite used in this study was obtained from Union Carbide (LZY-52). The benzene–NaY zeolite samples were prepared in 8-mm Pyrex tubes connected to a vacuum apparatus through a Teflon high-vacuum stopcock. Before addition of the adsorbate species, the NaY samples were dehydrated by heating at 723 K under vacuum (ca. 10^{-5} Torr) overnight. Adsorbate loadings were calculated with mass balances using NaY supercage density and the masses of zeolite and benzene. Benzene was initially introduced to the dehydrated NaY zeolite samples at room temperature in a glovebox filled with dry nitrogen gas. The samples were then placed in a furnace equipped with a programmable temperature controller, heated for 4 h at 523 K, and cooled to room temperature over a period of $^1/_2$ h. Each sample was reevacuated, at 77 K to prevent any desorption, after which oxygen gas was introduced to shorten the spin–lattice (T_1) relaxation times of adsorbed benzene at reduced temperatures.

MQ NMR in solids has been described in detail elsewhere,[15,16] so we limit ourselves to a brief outline of the experimental technique pertinent to this work. Proton multiple-quantum spectra were obtained on a home-built NMR spectrometer operating at 179 MHz. All spectra were obtained with the sample cooled by cold N_2 gas to an equilibrium temperature of 190 ± 1 K. The radio-frequency pulse sequence of Baum and Pines[17] was used and included the use of phase cycling and a pulse sequence cycle time of 60 μs. This pulse sequence creates a two-quantum average Hamiltonian

$$H = -\tfrac{1}{2}\sum D_{ij}(I_{i+}I_{j+} - I_{i-}I_{j-}) \qquad (1)$$

where I_+ and I_- are raising and lowering angular momentum operators. This Hamiltonian allows even-order MQ coherences to develop, with different MQ orders separated from each other by time proportional phase incrementation (TPPI).[18] A phase increment of $\pi/16$ rad allows observation of MQ transitions with $-16 \le \Delta m \le 16$, where Δm is the change in the spin quantum number m.

The two-dimensional MQ experiment is divided into four time periods: preparation, evolution, mixing, and detection. Spin networks are allowed to evolve and grow under the two-quantum Hamiltonian during the preparation period. Separation of the various MQ orders is achieved by a phase shift (TPPI) during the evolution period. The mixing period creates an average Hamiltonian that is equal, but opposite in sign, to the two-quantum Hamiltonian produced during the preparation work. This results in so-called "time-reversed" evolution of the spin network which refocuses the magnetization along the z axis. The intensity of the signal is observed during the detection period by tipping the magnetization and spin-locking. Plotting the magnitude of the magnetization vector as a function of phase shift creates the MQ

† Present address: Department of Chemistry, 47 Noyes Laboratory, University of Illinois at Urbana-Champaign, 505 South Mathews Ave., Urbana, IL 61801.

‡ Present address: Department of Chemical and Nuclear Engineering, University of California, Santa Barbara, CA 93106.

§ Present address: Quantum Design, 11578 Sorrento Valley Rd., Suite 30, San Diego, CA 92121.

0022-3654/92/2096-8517$03.00/0 © 1992 American Chemical Society

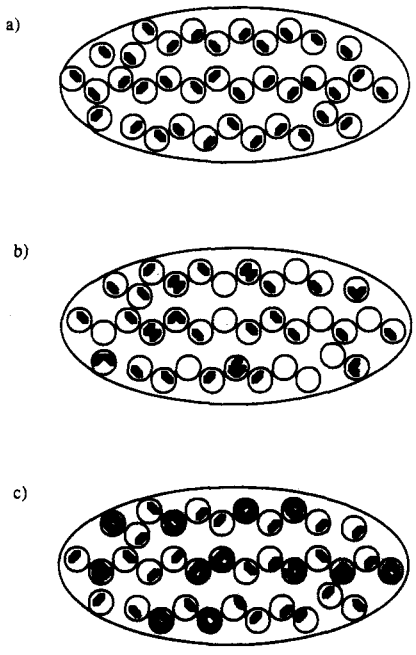

Figure 1. Diagrams of possible benzene distributions in NaY zeolite. The circles represent supercages, and the filled polygons represent benzene molecules. Parts a and b represent uniform and random distributions, respectively, for a bulk loading of one benzene guest per supercage. Part c depicts aggregation of molecules for a bulk loading of two guests per supercage.

interferogram. Fourier transformation of the interferogram generates the MQ spectrum, which is a function of the Hamiltonian created during the preparation period, the duration of the preparation period, and the properties of the spin networks present within the sample.

Results

The growth rate of a spin network under a two-quantum Hamiltonian is a function of both the number of like spins dipole–dipole coupled to the network and the magnitudes of these couplings. Growth of a spin network is limited, however, by the size of the dipole–dipole coupled spin cluster. In some systems, isolation of molecular species imposes finite upper bounds upon the size of proton spin clusters. For example, isolated clusters have been observed in samples of hexamethylbenzene adsorbed in NaY zeolite[13] and in nematic liquid crystals.[17] The former is an example of spatial isolation, while the latter is an example of isolation by motional quenching of intermolecular dipole–dipole couplings.

The limiting effect of isolation can be directly observed in the multiple-quantum spectra of a system. Figure 2 shows phase-cycled MQ NMR spectra of NaY zeolite containing a bulk average loading of two benzene molecules per supercage. Note that the widths of the spectra increase with increasing preparation time until a limit is reached at about 540 μs. Spectra acquired with preparation times greater than 540 μs are essentially identical, indicating that the spin network ceases to grow at longer preparation times. Such behavior demonstrates the presence of isolated spin clusters.

To measure the size of a spin cluster, we examine the relative peak intensities in each multiple-quantum spectrum. By determining the average size of the spin networks associated with each spectrum, the spin network size can be plotted as a function of preparation time. A plateau in such a plot would indicate the average size of isolated dipole–dipole coupled proton clusters, providing a direct measurement of the average number of benzene molecules present in each molecular cluster. It has been shown[19] that a spin network of N like-spins will generate a multiple-quantum spectrum with peak intensities closely approximated by the Gaussian expression

$$I(\Delta m) = A \exp(-(\Delta m)^2/N) \qquad (2)$$

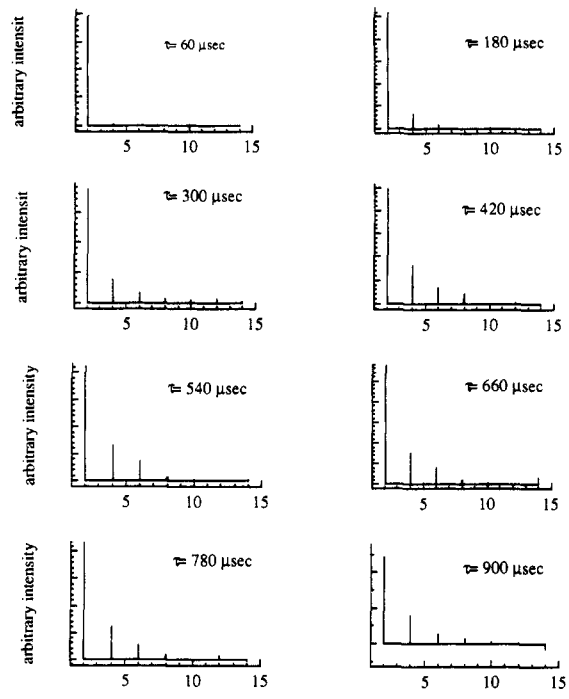

Figure 2. MQ spectra of NaY zeolite with a bulk loading of two benzene molecules per supercage. The preparation time t_p was varied from 60 to 900 μs.

where Δm is the order of the multiple-quantum transition, A is a constant, and $N - \Delta m$ is large enough to justify Stirling's approximation. The apparent average size of the spin networks in a sample is determined experimentally by fitting eq 2 to each MQ spectrum to find N, varying both A and N.

In general, the MQ spectra of benzene in NaY zeolite evolve with preparation time in a manner consistent with the presence of spin clusters corresponding to clusters of adsorbate molecules in the zeolite supercages. Our earlier study of hexamethylbenzene (HMB) adsorbed in NaY zeolite[13] showed the $\Delta m = 2$ transition for the HMB/NaY system to be unexpectedly intense. This may be due to the presence of strongly coupled methyl-group proton spins in HMB, which allow the proton spin networks within each supercage to evolve as either clusters of 18 spins or weakly coupled three-spin clusters, depending upon the local orientation of a HMB molecule with respect to the external magnetic field. The MQ spectra of HMB in NaY zeolite indicate a mixture of spin assemblies corresponding to HMB molecular clusters and much smaller, most likely intramolecular, spin clusters containing four or fewer spins. No evidence for such an intramolecular mixture of cluster sizes is observed in the MQ spectra of benzene adsorbed in NaY zeolite, possibly because benzene proton spins are able to evolve only in networks corresponding to molecular benzene clusters.

Figure 3a shows the average size of the spin network as a function of preparation time, $N(t_p)$, for NaY zeolite samples containing bulk average benzene loadings of one-half molecule and one molecule per supercage. Note that the average size of the spin network rises rapidly to a limit and then remains constant in both cases. The use of Stirling's approximation in the derivation of eq 2 will cause the observed value of N to be somewhat depressed for these two lowest loaded samples, but the difference between the observed cluster sizes for the two samples indicates a definite increase in the average number of benzene molecules per occupied supercage as the concentration of benzene is raised from a bulk average of one molecule per two supercages to one molecule per supercage. The limit reached by the spin network in the one-half benzene per supercage sample thus corresponds to an average molecular cluster size of one molecule per occupied supercage, consistent with half of all supercages in the sample containing a single benzene guest and half the supercages being empty. Since the diffusivity of benzene in NaY at the preparation temperature of 523 K is sufficiently high enough to distribute

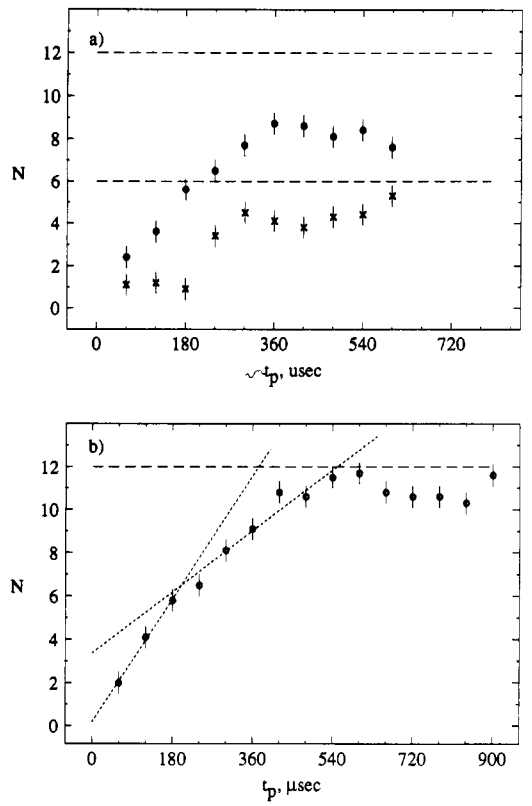

Figure 3. (a) Average spin network size as a function of preparation time, $N(t_p)$, for NaY zeolite with bulk loadings of one-half (×) and one (○) benzene molecule per supercage. (b) Average spin network size as a function of preparation time, $N(t_p)$, for NaY zeolite with a bulk loading of two benzene molecules per supercage. Dotted lines represent spin network growth rates observed before the cluster limit is reached. The long-dashed line corresponds to the spin network limit anticipated for a molecular cluster of two molecules per occupied supercage.

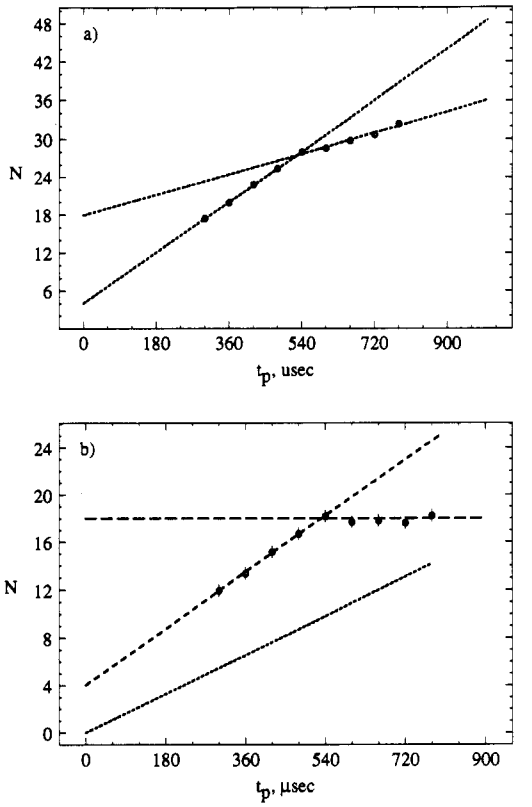

Figure 4. (a) Average spin network size as a function of preparation time, $N(t_p)$, for NaY zeolite with a bulk loading of three benzene molecules per supercage. (b) The same data with the influence of the *inter*supercage dipole–dipole couplings removed. The long-dashed line corresponds to the spin network limit anticipated for a molecular cluster of three molecules per occupied supercage.

benzene molecules throughout the NaY crystallite,[20] the observed molecular cluster size of one benzene molecule per supercage is supportive of an essentially uniform distribution of benzene throughout the zeolite.

The spin limit reached by the sample with a bulk loading of one molecule per supercage corresponds to an average of ~1.5 benzene molecules per occupied supercage, indicating a mixture of cluster sizes. Such a mixture requires that some supercages remain empty, raising the average cluster size measured since empty supercages do not contribute to the signal. A distribution of cluster sizes may be caused by a random distribution of benzene molecules among the supercages, or it may be caused by the formation of a few large aggregates surrounded by an otherwise uniform distribution of benzene molecules at lower concentration. Increasing the benzene loading in NaY zeolite should allow us to differentiate between random and aggregated cluster distributions. Large aggregations of benzene guest molecules in NaY supercages, for example, will produce significantly larger average spin network sizes than those arising from a random distribution of adsorbed benzene guests.

Figure 3b shows the average size of the spin networks as a function of preparation time, $N(t_p)$, for a NaY zeolite sample with a bulk loading of two benzene molecules per supercage. The size of the spin network grows rapidly for the first 180 μs and then continues to grow at a slower rate until the cluster size is reached at ~540 μs. The period of rapid growth (<200 μs) corresponds to the correlation of ^{1}H spins within individual benzene molecules via the relatively strong intramolecular homonuclear dipole–dipole couplings. The slower growth after ~200 μs is the result of the weaker dipole–dipole couplings between spin networks on different benzene molecules in the same supercage. The spin network size limit corresponds to an average molecular cluster size of about two molecules per occupied supercage. Both random and uniform distributions of benzene molecules within the zeolite can account for this behavior. As noted above, the presence of large molecular aggregates would be indicated by a noticeably higher average cluster size than that observed. This apparently rules out the formation of relatively large benzene aggregates at low guest loadings.

Further increases in the benzene loading should reveal the effects of molecular competition for the cation adsorption sites, since loadings of more than two benzene molecules per cage will occupy more than half of these sites. Figure 4a is a plot of the average spin network size as a function of preparation time, $N(t_p)$, for a NaY zeolite sample with a bulk loading of three benzene molecules per supercage. The spin network grows at a constant rate over the interval 300 μs ≤ t_p ≤ 540 μs and then grows at a slower constant rate, from 540 μs to the end of our experimental range. The dotted lines were determined by a linear least-squares fit to the respective regions of the $N(t_p)$ curve. As in Figure 3b, the growth rate of the spin network for t_p ≤ 540 μs is dominated by the coupling of spins within the same supercage. However, for three benzene molecules per supercage the guest density is sufficiently high that separate periods of spin network growth arising from *intra*- and *inter*molecular dipole–dipole couplings cannot be distinguished. The growth rate of the spin network after 540 μs is likely due to the coupling of spins in neighboring supercages, since the size of the spin network shows no upper limit.

Large differences in dipole–dipole couplings between *intra*- and *inter*supercage proton pairs permit us to determine the relative spin network growth rates that arise from these dipole–dipole couplings. The contribution from *inter*supercage dipole–dipole couplings to the growth rate of the spin network is found by examining the slope of the $N(t_p)$ curve above 540 μs, since the spin network growth at this point is due primarily to *inter*supercage couplings. Since the growth of a spin network's size under a given dipole–dipole coupling strength is linear in time,[19] the contribution from *inter*supercage couplings can be modeled as a line passing through the origin and having a slope identical to that of the $N(t_p)$ curve above 540 μs. Subtracting this line from the $N(t_p)$ curve

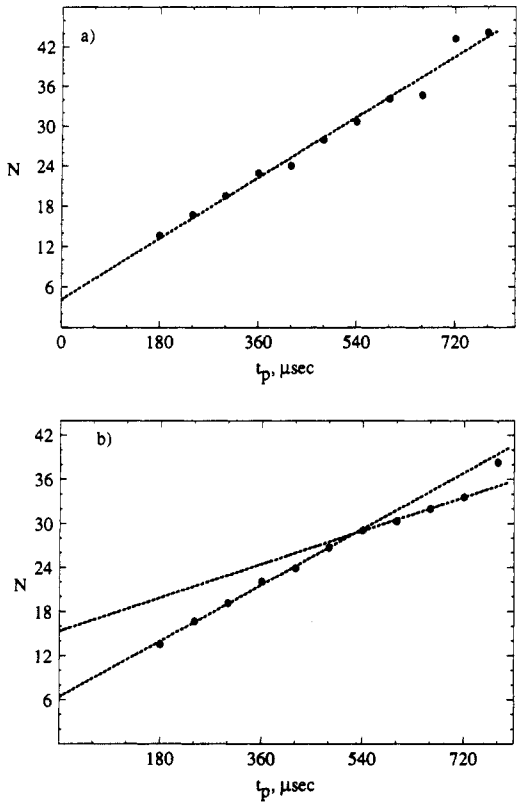

Figure 5. (a) Average spin network size as a function of preparation time, $N(t_p)$, for NaY zeolite with a bulk loading of four benzene molecules per supercage. (b) The same data with the contribution of the continuous spin network removed. A least-squares fit of data for 540 μs $\leq t_p \leq$ 720 μs intercepts the y axis at ~15 spins.

removes the *inter*supercage dipole–dipole contribution to the evolution of the spin network, leaving only the contribution due to the *intra*supercage dipole–dipole couplings. Figure 4b is a plot of the difference between the data shown in Figure 4a and a line passing through the origin with a slope identical to that of the least-squares fit to the data for preparation times (t_p) greater than or equal to 540 μs. The curve shown in Figure 4b therefore represents the evolution of the spin networks decoupled from the effects of molecules in neighboring supercages. The cluster limit of the spin network (18 spins) within the supercage corresponds to three benzene molecules per occupied supercage, consistent with a uniform distribution of benzene molecules among the zeolite supercages. Both a random molecular distribution and a model based upon preferential aggregation of benzene guests would generate higher average spin cluster sizes, and thus these distribution models appear unlikely.

As the density of adsorbed benzene in NaY zeolite is increased, the size of the coupled spin system becomes larger as well. Figure 5a is a plot of $N(t_p)$ for a NaY zeolite sample with a bulk loading of four benzene molecules per supercage. The absence of any limit on the spin network size N or any obvious decrease in the spin network's growth rate is characteristic of an essentially infinite collection of coupled spins. This occurs when there is little or no difference in the magnitude of dipole–dipole couplings between spins or groups of spins within a sample. In the case of benzene in NaY zeolite, this reflects a lack of spatial isolation among benzene molecules adsorbed in adjacent supercages. Inspection of the MQ spectra obtained at long preparation times shows the peak intensities to be the sum of two Gaussians: one that is approximately the same width as for the sample containing three benzene molecules per supercage and another that is much broader. This reflects a clustered spin network mixed with a continuous spin network. We assume that the size of the continuous spin network is much larger than that of the clustered spin network. This assumption allows us to discount the influence of the continuous spin network from the MQ spectra by subtracting the height of an "infinitely" wide Gaussian from each

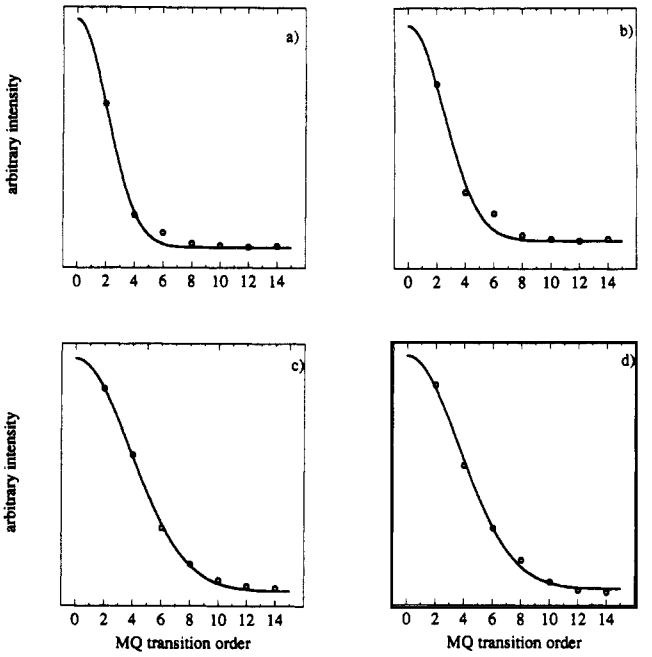

Figure 6. MQ spectra with preparation times t_p of 600 μs for NaY zeolite with bulk loadings of (a) one molecule per supercage, (b) two molecules per supercage, (c) three molecules per supercage, and (d) four molecules per supercage.

of the peak intensities. This is done by incorporating a constant offset parameter into the Gaussian-fit program, thereby shifting the Gaussian curve to account for the continuous spin network's contribution to each spectrum. Figure 5b displays the average size of the spin network as a function of preparation time, $N(t_p)$, after removing the contribution of the continuous spin network from each spectrum. The values of $N(t_p)$ are essentially the same as in Figure 5a until $t_p \sim$ 540 μs, at which point the diminished slope of the plot reflects a lessening of the spin network growth rate. This is characteristic of weakly coupled clusters, as shown previously (Figure 4a), for a bulk loading of three benzene molecules per supercage.

At high guest loadings, it is furthermore possible to investigate competitive adsorption of benzene at different zeolite sites. The continuous spin network, for example, is most likely the result of a significant number of benzene molecules occupying window sites (W) between two adjacent supercages. Sample loadings above three benzene molecules per cage can trap molecules in energetically less favorable window positions through prior occupation of the adjacent cation sites (S_{II}). The magnitude of the intermolecular dipole–dipole couplings would be approximately the same throughout such a continuous spin network because molecules in W sites bridge the gaps between adjacent supercages.

To help distinguish between the uniform and random guest distribution possibilities, we examine the MQ spectra of each system at sufficiently long preparation times such that the spins on benzene molecules in the same supercage have reached the cluster limit. Each spin cluster contributes signal to a spectrum according to eq 2; that is, each spin contributes signal to the MQ peak intensities in the form of an approximately Gaussian distribution. A random distribution of molecules among zeolite supercages will generate MQ spectra with peak intensities that approximate a sum of Gaussian distributions, with each different cluster size contributing to the total signal. For example, the MQ spectra of NaY zeolite with a bulk loading of one benzene molecule per supercage is expected to exhibit such behavior, for we have determined from our analysis that this system contains a mixture of molecular cluster sizes.

We show the results of such comparisons in Figure 6 for NaY samples containing guest loadings of 1–4 benzene molecules per supercage. In all four cases the preparation time (t_p) is 600 μs. The MQ spectra from samples with one or two benzene molecules per supercage are not well approximated by a least-squares

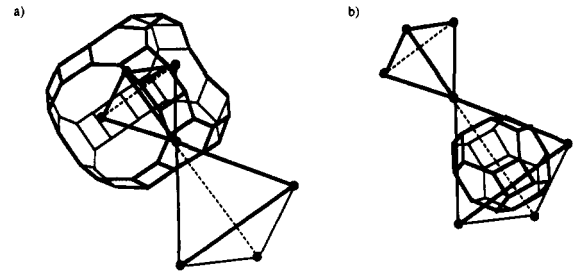

Figure 7. Diagram of the proposed site geometry for benzene molecules adsorbed in NaY zeolite supercages. The small tetrahedron is contained within a supercage, and the large tetrahedron envelops a sodalite cage. The ratio of the tetrahedras' edges is 1:1.6.

Guassian fit (R^2 values of 0.992 and 0.984, respectively), indicating the presence of more than one spin cluster size in the sample. At low loadings, therefore, there apparently exists a mixture of cluster sizes, consistent with a random distribution of benzene guests adsorbed at 523 K. For higher benzene loadings of 3–4 molecules per supercage, however, the MQ spectra are closely approximated by single Gaussian functions (R^2 values of 0.999 and 0.998, respectively), supporting a more uniform distribution of the adsorbed guests.

The relative configuration of the adsorbate molecules within the zeolite supercages can also be inferred from the spin network growth rates measured when weakly coupled clusters are observed. The growth rate of a spin network is approximately proportional to the product of the mean dipolar line width and the number of spins being incorporated into the network.[19] The relative dipolar coupling strengths involved in each of the growth mechanisms can therefore be found by dividing each slope by the number of spins in the respective subnetworks, in this case six, for a single benzene molecule, and 18, for a three-molecule cluster in a supercage

$$|D_1|/|D_2| \approx (m_1/6)/(m_2/18) = 4.3 \qquad (3)$$

where the D_i's are the respective dipole couplings and the m_i's are the growth rates (slopes). To calculate the distances between spins on different benzene molecules, we note that benzene adsorbed in NaY zeolite rotates rapidly about its 6-fold axis at temperatures between 125 and 250 K,[5] allowing us to treat the center of each benzene molecule as a group of six protons. The ratio of distances between molecular centers within the same supercage and between those in adjacent supercages can be approximated by taking the cube root of the relative dipolar coupling strength estimated from eq 3. This indicates relative benzene–benzene distances of ~1:1.6 between benzene molecules adsorbed in the same supercage and benzene molecules adsorbed in adjacent supercages.

Assuming benzene guests adsorb at S_{II} sites within the zeolite and also assuming an average displacement from the Na^+ ion of about 3 Å,[4,8,21,22] we find the above results to be consistent with molecular centers arranged on the vertices of two sets of tetrahedra, as shown in Figure 7. The edges of the smaller tetrahedra represent the distances between molecular centers within the *same* supercage, while the edges of the larger tetrahedra represent the distances between the nearest molecular centers in *adjacent* supercages. NaY sodalite cages are located within the large tetrahedra, about 3 Å from the vertices. Since the supercages are ~13 Å across, this model reflects an outer diameter for the sodalite cage of ~10 Å. This is consistent with the symmetry and lattice parameters of the sodalite structure obtained from diffraction experiments[23] after accounting for the finite dimensions of the sodalite cage's constituent atoms. This supports our assumption that the benzene molecules occupy only the cationic (S_{II}) sites in the NaY zeolite supercages at this loading, since occupation of different types of sites would generate different dipole coupling ratios from those observed.

Discussion

On the basis of our MQ NMR results, we postulate a loading-dependent distribution model for benzene molecules adsorbed on NaY zeolite. As benzene is introduced to dehydrated NaY zeolite at 523 K, the dilute guest molecules diffuse freely between the supercages, adsorbing at, and hopping between, cationic sites (S_{II}) randomly. The absence of uniform or aggregated benzene distributions at low loadings shows no exclusionary effects against multiply occupied supercages and reflects no preferred molecular cluster size. For a bulk loading of three benzene molecules per supercage, however, the essentially uniform distribution of guest species demonstrates a preference against adsorption of four benzene molecules per supercage. The clear bimodal behavior of the spin network growth rate indicates the existence of only two distances for guest–guest separation, confirming predominant occupation of S_{II} sites at this loading. Adsorbing benzene molecules at all four S_{II} sites within a supercage appears to be sufficiently unfavorable that a large number of benzene molecules are directed to window sites (W), as evidenced by the continuous spin network observed in NaY zeolite with a bulk loading of four molecules per supercage. There are half as many W sites as S_{II} cation sites, since each of the four windows adjoining a supercage is shared with a neighboring supercage. An extrapolation of the linear least-squares fit of the >540-μs region of Figure 5b leads us to believe that the only supercages without at least one W site occupied are those that have only three or fewer S_{II} sites occupied by benzene guests. Bulk loadings of more than four benzene molecules per supercage generate an essentially infinite spin network and therefore could not be investigated using MQ NMR. It is reasonable that additional molecules, up to the maximum sorption capacity of 5.4 molecules per supercage, probably fill the remaining S_{II} and W sites, as has been previously suggested.[2-4]

Conclusions

The technique of MQ NMR allows the size of spin networks to be established through examination of the behavior of groups of spins evolving under a two-quantum Hamiltonian. By determining spin cluster sizes, molecular populations in isolated cavities can be probed, with the growth rate of the spin networks reflecting the configuration of the adsorbed species in the sample.

We have used MQ NMR to develop a model for the distribution of benzene adsorbed on NaY zeolite. Guest benzene molecules appear to adsorb randomly at available cationic (S_{II}) sites for loadings of less than three molecules per supercage. The distribution becomes uniform as the loading approaches three benzene guests per supercage, reflecting a barrier to guest occupation of all four S_{II} sites in a supercage. Adsorption at the energetically less favorable window sites (W) is evidenced by the creation of continuous spin networks only in NaY samples containing four benzene molecules per supercage, again indicating a barrier to guest occupation of all four S_{II} sites in a supercage.

Acknowledgment. This work was supported by the Director, Office of Energy Research, Office of Basic Energy Sciences, Materials Sciences Division of the U.S. Department of Energy, under Contract DE-AC03-76SF00098. B.F.C. acknowledges funding as an NSF Postdoctoral Fellow in Chemistry.

Registry No. Benzene, 71-43-2.

References and Notes

(1) Lechert, H.; Hennig, H. *Z. Naturforsch., Teil A* **1974**, *29*, 1065.
(2) de Mallmann, A.; Barthomeuf, D. *New Developments in Zeolite Science and Technology*. Presented at the 7th International Zeolite Conference, Tokyo, 1986.
(3) Lechert, H.; Wittern, K.-P.; Schweitzer, W. *Acta Phys. Chem.* **1978**, *24*, 201.
(4) Lechert, H.; Wittern, K.-P. *Ber. Bunsen-Ges. Phys. Chem.* **1978**, *82*, 1054.
(5) Zibrowius, B.; Caro, J.; Pfeifer, H. *J. Chem. Soc., Faraday Trans. 1* **1988**, *84*, 2347.
(6) Renouprez, A. J.; Jobic, H.; Oberthür, R. C. *Zeolites* **1985**, *5*, 222.
(7) Fitch, A. N.; Jobic, H.; Renouprez, A. J. *J. Chem. Soc., Chem. Commun.* **1985**, 284.
(8) Germanus, A.; Kärger, J.; Pfeifer, H.; Samulevic, N. N.; Zdanov, S. P. *Zeolites* **1985**, *5*, 91.
(9) Newsam, J. M.; Silbernagel, B. G.; Garcia, A. R.; Hulme, R. *J. Chem. Soc., Chem. Commun.* **1987**, 664.
(10) Taylor, J. C. *Zeolites* **1987**, *7*, 311.
(11) Demontis, P.; Yashonath, S.; Klein, M. C. *J. Phys. Chem.* **1989**, *93*, 5016.

(12) O'Malley, P. J. *Chem. Phys. Lett.* **1990**, *166*, 340.
(13) Chmelka, B. F.; Pearson, J. G.; Liu, S. B.; Ryoo, R.; de Menorval, L. C.; Pines, A. *J. Phys. Chem.* **1991**, *95*, 303.
(14) Liu, S. B.; Wu, J. F.; Ma, L.; Lin, M. W.; Chen, T. L. Presented at the ACS National Meeting, Aug 25-30, New York, 1991.
(15) Baum, J.; Munowitz, M.; Garroway, A. N.; Pines, A. *J. Chem. Phys.* **1985**, *83*, 2015.
(16) Yen, Y. S.; Pines, A. *J. Chem. Phys.* **1983**, *78*, 3579.
(17) Baum, J.; Pines, A. *J. Am. Chem. Soc.* **1986**, *108*, 7447.
(18) Drobney, G.; Pines, A.; Sinton, S.; Weitekamp, D. P.; Wemmer, D. *Faraday Symp. Chem. Soc.* **1979**, *13*, 49.
(19) Munowitz, M.; Pines, A.; Mehring, M. *J. Chem. Phys.* **1987**, *86*, 3172.
(20) Foerste, C.; Kaerger, J.; Pfeifer, H. *Zeolites: Facts, Figures, Future, Studies in Surface Science and Catalysis*; Elsevier: Amsterdam, 1989; Vol. 49A, p 907. Chmelka, B. F.; Gillis, J. V.; Petersen, E. E.; Radke, C. J. *AIChE J.* **1990**, *36*, 1562.
(21) Hoffmann, W.-D. *Z. Phys. Chem. (Leipzig)* **1976**, *257*, 315.
(22) Loeffler, A.; Penker, C.; Kunath, D. *Adsorption of Hydrocarbons-II*; workshop Eberswalde 1982, supplement.
(23) Meier, W.; Olson, D. H. *Atlas of Zeolite Structure Types*; Butterworths: London, 1987.

Influence of TiO_2 Surface on 1,2-Chlorine Shift in β-Chlorine Substituted Radicals As Studied by Radiation Chemistry and Photocatalysis

Yun Mao,† Christian Schöneich,‡ and Klaus-Dieter Asmus*

Hahn-Meitner Institut Berlin GmbH, Bereich S, Abteilung Strahlenchemie, Postfach 39 01 28, W-1000 Berlin 39, Germany *(Received: April 21, 1992; In Final Form: July 14, 1992)*

The influence of surface-specific parameters on the photocatalytically induced oxidative degradation of halogenated hydrocarbons in aqueous TiO_2 suspensions has been evaluated by comparing the results obtained in this heterogeneous system with those from γ-irradiated homogeneous aqueous solutions. A 1,2-chlorine shift known to occur in β-chlorinated alkyl radicals and the products obtained upon degradation of these radicals (particularly various chloroacetic acids) have been used as markers in these investigations. The results indicated that this chlorine shift, e.g., the rearrangement of $CCl_3-CH_2^{\bullet} \rightarrow {}^{\bullet}CCl_2-CH_2Cl$, occurs much slower ($k$ in the order of 10^6 s^{-1}) at the TiO_2 surface than in the homogeneous solution, where the present data confirm earlier rate constants of $\geq 10^8$ s^{-1}. This slowdown of the rearrangement process is attributed to steric hindrance in the surface-adsorbed state of the radicals. In the heterogeneous systems the rearrangement can, in fact, be interfered with by peroxidation of the unrearranged radical in the presence of molecular oxygen while such a competition cannot be achieved in the homogeneous solution even at high O_2 concentrations. Experimentally, this has been demonstrated, for example, by the fate of the ${}^{\bullet}CHCl-CCl_3$ radical generated upon oxidative C-H cleavage from 1,1,1,2-tetrachloroethane. Direct oxygen addition to this species yields the ${}^{\bullet}OOCHCl-CCl_3$ peroxyl radical which eventually degrades into CCl_3COOH. After rearrangement (${}^{\bullet}CHCl-CCl_3 \rightarrow CHCl_2-CCl_2{}^{\bullet}$) and subsequent peroxidation the then formed $CHCl_2-CCl_2OO^{\bullet}$ peroxyl radical ends up in a completely different acid, namely, $CHCl_2COOH$. It could further be deduced that the 1,2-chlorine shift occurs via a bridged mechanism without transient liberation of the chlorine atom, thereby rendering an alternatively possible chlorine elimination/readdition mechanism an unlikely event. Finally, a marked pH dependence of the product distribution in both the γ-radiolytic and photocatalytic system is suggested to reflect acid/base catalyzed hydrolysis processes en route of the radical degradation to their final products.

Introduction

The redox-initiated degradation of halogenated organic compounds is known to generally proceed via free-radical mechanisms. This has been demonstrated, for example, for the biochemical process of metabolism[1] and many radiation chemical studies.[2-14] The involvement of radicals has also been implied in a recent detailed study on the photocatalytic degradation of such substrates en route to mineralization.[15] The fact that, for example, chlorinated organic compounds are ultimately degraded into CO_2 and HCl upon photocatalysis has already been shown in many earlier investigations.[16-33] This latter aspect is, of course, of particular interest in view of the environmental hazard most halogenated organic compounds represent. The underlying chemistry can be rationalized on the basis of the redox processes initiated upon illumination of semiconducting material.[34-51]

The involvement of radicals appears to apply already for the early steps in a photocatalytic process. For the oxidation of substrates at TiO_2 surfaces, for example, the question had been raised whether this proceeds directly by valence band holes or goes through an intermediary formation of surface adsorbed hydroxyl radicals.[34-48] In our recent study on the oxidative degradation of chlorinated ethanes[15] we could provide good supporting evidence that the initiating step was indeed the generation of adsorbed hydroxyl radicals

$$\equiv Ti-OH^- + h_{VB}^+ \rightarrow \equiv Ti-{}^{\bullet}OH \quad [{}^{\bullet}OH_{ads}] \qquad (1)$$

which preceded the actual oxidation of the substrate

$$>C(Cl)-C(H)< + {}^{\bullet}OH_{ads} \rightarrow >C(Cl)-C^{\bullet}< + H_2O \qquad (2)$$

Only when the organic compounds did not provide suitable C-H bonds for this hydrogen abstraction process could the oxidation occur through the, energetically apparently less favorable, direct valence band hole reaction.[15,33]

Assignment of the underlying radical mechanism of the mineralization process became possible by comparison of the photocatalytic results with those from γ-radiolysis. The suitability of this complementary approach, in general, has been pointed out already in a number of cases.[28,35,49-51] In our particular system the γ-radiolytic oxidation of the halogenated compounds occurs in analogy to reaction 2, although with freely diffusing hydroxyl radicals.[10,15] Rationalization of the overall mechanism has in particular been based on the qualitative identity of the products generated by these two complementary methods: organic acids, aldehydes, fragmentation products, CO_2, and HCl. The formation of all these products can directly be related to and understood in terms of the well-known and documented chemistry of peroxyl radicals, in general.[52,53]

† Present address: Department of Chemistry and Biochemistry, University of Notre Dame, IN 46556.
‡ Present address: Department of Pharmaceutical Chemistry, University of Kansas, Lawrence, KS 66045.

0022-3654/92/2096-8522$03.00/0 © 1992 American Chemical Society